*M&C 2017 - International Conference on Mathematics & Computational Methods Applied to Nuclear Science & Engineering, Jeju, Korea, April 16-20, 2017, on USB (2017)*

# A New Tone's Method in APOLLO3® and its Application to ZPPR Benchmarks

Li Mao, Igor Zmijarevic

*CEA-Saclay, DEN, DM2S, SERMA, F-91191 Gif-sur-Yvette, France*
*li.leimao@cea.fr, igor.zmijarevic@cea.fr*

**Abstract** - *This paper presents a newly developed resonance self-shielding method based on Tone's method in APOLLO3® for fast reactor calculations. The new method is based on the simplified models, the narrow resonance approximation for the slowing down source and Tone's approximation for group collision probability matrix. It utilizes the mathematical probability tables as quadrature formulas in calculating the effective cross sections. Numerical results for the ZPPR drawer calculations show that, in case of the double column fuel drawer, Tone's method gives equivalent precision to the subgroup method while reducing largely the total number of the collision probability matrix calculations hence the CPU time. In case of the single column fuel drawer with presence of a uranium metal material, Tone's method obtains less precise results than those of the subgroup method due to less precise heterogeneous-homogeneous equivalence.*

## I. INTRODUCTION

In reactor lattice analysis, the aim of resonance self-shielding calculation is to estimate the group-averaged cross sections for solution of the multigroup transport equation. The accuracy of the resulting group parameters determines the precision of multigroup calculation.

For the fast reactor analysis with the APOLLO3® [1, 2] code, a subgroup (SG) method based on the ECCO formalism was implemented [3, 4]. This method utilizes the mathematical probability tables based on the CALENDF formalism [5] provided by the GALILEE project [6]. Different from the other self-shielding methods which make simplified assumptions on the source term, this subgroup method directly employs the multigroup neutron sources in self-shielding procedure, hence no assumption is made on the source term. This is achieved by embedding the self-shielding calculation in multigroup flux calculation. The numerical tests showed the accuracy of the subgroup method with a 1968-group energy mesh in sodium-cooled fast reactor analysis [4] compared to TRIPOLI-4® Monte Carlo continuous-energy reference [7]. However it was also showed that the APOLLO3® subgroup method consumed important CPU time. This method deals with the resonant interference effects approximately using Bondarenko iteration. The effects of a temperature distribution are approximately calculated by assuming that all isotopes of the same type are at the same temperature than those in the region being treated.

In this work, a new resonance self-shielding method based on Tone's method [8] has been developed in APOLLO3®, in order to reduce the running time while keeping similar calculation precision. This method has been traditionally applied to fast reactor analysis [9] with fine or ultrafine group energy mesh. It is based on the heterogeneous-homogeneous equivalence. However, unlike the traditional equivalence theory, Tone's method determines the equivalent cross sections using a set of group collision probabilities [8], or by the solution of two fixed-source transport equations [10, 11]. By employing the transport solvers available in APOLLO3®, such as the collision probability (CP) method, the finite difference and finite element methods, or the short and long method of characteristics (MOC), which can be applied to structured or unstructured geometries, Tone's method is available for all geometries supported by the solvers. This lifts the limitation of the traditional equivalence theory, which is based on Wigner's rational approximation of the fuel-to-fuel collision probability [12] and limited to fuel cell or regular lattice of fuel cells. Dancoff factors [13] and Bell corrections can be utilized to extend the method to more general systems, but they are difficult to calculate for arbitrary geometries.

When the equivalent cross sections have been determined, the mathematical probability tables [5] are utilized as quadrature formulas to compute the effective cross sections. This is different from the precedent studies [14, 10, 11], where the self-shielded cross sections were determined either by interpolation from the pretabulated effective cross sections for the infinite homogeneous medium (IHM), or by employing the ultrafine group cross sections (~400,000 groups). We believe that the utilization of probability tables offers an important advantage over preceding practices: the calculation with probability tables is precise and fast; the probability tables use very little memory; there is no need to pretabulate IHM effective cross sections. In unresolved resonance range, the probability tables are suitable for describing the statistical behavior of the resonances. In resolved resonance range, the probability tables with a fine or ultrafine mesh are capable to preserve the original cross sections with a high precision. The first numerical results showed that Tone's method has nearly the same precision as the subgroup method for typical sodium fast reactor (SFR) calculations, while the CPU time is dramatically reduced [4]. In this paper, the new Tone's method is applied to the ZPPR benchmark calculations [15]. The numerical results are compared to those of the TRIPOLI-4® Monte Carlo continuous-energy calculations and to those of the subgroup method.

The rest of paper is organized as follows. In Section II we present the theory of Tone's method and its implementation. In Section III we present numerical results of the ZPPR benchmark calculations using Tone's method and the subgroup method, by taking the continuous energy TRIPOLI-4® Monte Carlo calculations as references. Conclusions are drawn in the final section.

## II. TONE'S METHOD

In this work, interference effects introduced by mixtures of resonant isotopes are treated by Bondarenko iterations. The resonant isotope is treated individually by using the group cross sections for the other resonant isotopes.

In situation of an infinite homogeneous medium consisting of a resonant isotope $x$ and other isotopes considered as moderators, the neutron flux is written as follows

$$\Phi(u) = \frac{S(u)}{N_x\sigma_x(u) + \sum_{y\neq x} N_y\sigma_y(u)}, \tag{1}$$

where $S$ is the neutron source, $N$ is the number density, $\sigma$ is the microscopic total cross-section and $u = ln(E_0/E)$ is the lethargy. In fast spectrum reactor calculations, a fine or ultrafine energy meshes is conventionally employed. In this case, the narrow resonance (NR) approximation, $S(u) \approx \Sigma_p$, can be applied to all isotopes. The upper equation can be re-written as follows

$$\Phi(u) \approx \frac{C}{\sigma_x(u) + \sigma^g_{bx}}, \tag{2}$$

where $C$ is a constant and $\sigma^g_{bx} = \frac{1}{N_x}\sum_{y\neq x} N_y\sigma^g_y$ is the background cross-section for isotope $x$.

We consider next the heterogeneous situation. The CP formalism for a region $i$ is written as follows

$$V_i\Sigma_i(u)\Phi_i(u) = \sum_j P_{ij}(u)S_j(u)V_j, \tag{3}$$

where $V$ stands for region volume, $P_{ij}$ is the collision probability for a neutron born in region $j$ to undergo its first collision in region $i$ and $S$ is the source term. Tone's approximation [8], which supposes that the collision probability $P_{ij}$ as a function of lethargy depends only on the arrival region $i$, is written here as follows

$$P_{ij}(u) = f^g_i(u)P^g_{ij}. \tag{4}$$

Applying the reciprocity and conservation relations [16] for the collision probabilities,

$$V_i\Sigma_i(u)P_{ji}(u) = V_j\Sigma_j(u)P_{ij}(u), \tag{5}$$

$$\sum_j P_{ji}(u) = 1, \tag{6}$$

together with Tone's approximation and the NR approximation, we obtain

$$\Phi_i(u) \approx \frac{D}{\sum_j P^g_{ij}\Sigma_j(u)V_j}, \tag{7}$$

where $D$ is a constant.

When we carry out the self shielding of resonant isotope $x$, by writing the total cross section in region $j$ as

$$\Sigma_j(u) = N_{xj}\sigma_x(u) + \sum_{y\neq x} N_{yj}\sigma^g_{yj}, \tag{8}$$

Eq. (7) can be written as follows

$$\Phi_{xi}(u) \approx \frac{E}{\sigma_x(u) + \sigma^g_{0xi}}, \tag{9}$$

where $E$ is a constant and

$$\sigma^g_{0xi} = \frac{\sum_j P^g_{ij}V_j\sum_{y\neq x} N_{yj}\sigma^g_{yj}}{\sum_j P^g_{ij}V_jN_{xj}} \tag{10}$$

is the equivalent cross section for isotope $x$ in region $i$.

The formula shows that the equivalent cross section is the ratio of two region averaged scalar fluxes,

$$\sigma^g_{0xi} = \frac{\Phi^g_{1i}}{\Phi^g_{2i}}, \tag{11}$$

which can be obtained from two fixed-source equations in purely absorbing media

$$V_i\Sigma^g_i\Phi^g_{1i} = \sum_j P^g_{ij}V_j\sum_{y\neq x} N_{yj}\sigma^g_{yj}, \tag{12a}$$

$$V_i\Sigma^g_i\Phi^g_{2i} = \sum_j P^g_{ij}V_jN_{xj}. \tag{12b}$$

The analogy between Eq. (9) and Eq. (2) is the basis for heterogeneous-homogeneous equivalence. One region in a heterogeneous system can be considered as an infinite homogeneous medium with a characterizing background cross section defined by Eq. (10). In traditional equivalence theory [17], Eq. (9) is written as

$$\Phi_{xi}(u) = \frac{E}{\sigma_x(u) + \sigma^g_{bxi} + \sigma^g_{exi}}, \tag{13}$$

where $\sigma^g_{bxi} = \frac{1}{N_x}\sum_{y\neq x} N_y\sigma^g_{yi}$ is the background cross section in region $i$, and $\sigma^g_{exi} = \sigma^g_{0xi} - \sigma^g_{bxi}$ is the *escape cross section* which accounts for neutrons streaming through the region surface.

In preceding studies of Tone's method, the self-shielded cross-sections were computed by interpolating the IHM effective cross sections [14, 10] or by utilizing the ultrafine group cross sections (~400,000 groups) [11]. In our realization, the effective cross-sections are calculated by taking the mathematical probability table as quadrature formulas [5] and the flux in Eq. (9) as weighting spectrum. The probability tables are supplied by GALILEE project [6]. For a reaction $\rho$, the self-shielded cross-section is given by the formula

$$\sigma^g_{\rho xi} = \frac{\int_g \frac{\sigma_{\rho x}(u)}{\sigma_x(u) + \sigma^g_{0xi}}du}{\int_g \frac{1}{\sigma_x(u) + \sigma^g_{0xi}}du} \approx \frac{\sum_k \frac{p^g_{x,k}\sigma^g_{\rho x,k}}{\sigma^g_{x,k} + \sigma^g_{0xi}}}{\sum_k \frac{p^g_{x,k}}{\sigma^g_{x,k} + \sigma^g_{0xi}}}, \tag{14}$$

where

$$\{p^g_{x,k}, \sigma^g_{x,k}, \sigma^g_{\rho x,k}, k = 1, K^g\} \tag{15}$$

is the probability table for isotope $x$ in group $g$, with $\sigma^g_{x,k}$ and $p^g_{x,k}$ as abscissas and weights respectively, and $k$ is the

subgroup index and $K^g$ is the total number of subgroups. $\sigma^g_{\rho x,k}$ is the cross section for reaction $\rho$ associated to $\sigma^g_{x,k}$.

The self-shielded cross section depends on the equivalent cross section $\sigma^g_{0xi}$, which is in turn determined by the solution of the fixed-source Eqs. (12a) and (12b), where the self-shielded total cross sections are utilized to compute the group collision probabilities. Therefore iterations are necessary until convergence of the self-shielded cross sections for all resonant isotopes in mixture. In present implementation, the CP solver was employed in APOLLO3®, although coupling to other APOLLO3® solvers are also scheduled. Since the CP matrix computation is the most time-consuming part in self-shielding calculation, a Jacobi iteration was implemented to converge the self-shielded cross sections independently of the order of the resonant isotopes being treated.

For a given group, the iterations begin with the CP matrices calculation using the self-shielded cross sections from the last iteration. Then the equivalent cross sections $\sigma^g_{0xi}$ are determined by using Eq. (10) for each resonant isotope and region. Finally the new self-shielded cross sections $\sigma^g_{\rho xi}$ are computed by Eq. (14) using the newly obtained $\sigma^g_{0xi}$. The iterations continue until the desired convergence is achieved. The initial values for the microscopic self-shielded cross sections are often those corresponding to infinite dilution.

Consequently, the total number of collision probability calculations in one group is independent of the number of resonant isotopes being self-shielded, and equals the number of iterations.

## III. RESULTS AND ANALYSIS

The new Tone's method was first tested using the typical sodium-cooled fast reactor (SFR) fuel cell and assembly [4]. The numerical results showed Tone's method, compared to the subgroup method, gave equivalent precision for the effective multiplication factor and the reaction rates.

In this work, Tone's method was applied to the drawer calculations of the ZPPR benchmarks [15]. The ZPPR reactor is conceived as a matrix of steel plate drawers, which are composed of plates of different materials. The principal materials are plutonium alloys, uranium metal, uranium oxide, sodium and control rod absorbers. One of the particularities of ZPPR reactor is the ZPPR-Pu fuel composed of Pu-U-Mo alloy. Two types of fuel drawers, single column fuel (SCF) drawer and double column fuel (DCF) drawer, contain respectively one and two ZPPR-Pu plates. The inner core and outer core of ZPPR are mainly filled with the SCF and DCF drawers. The simplified geometry models of the SCF and DCF drawers are given in Fig. 1 and Fig. 2. One can find more details in [15].

The APOLLO3® calculations employed the ECCO 1968-group energy mesh [3] and use the CEA2005 V5.1 library. The translation boundary condition was adopted for both SCF and DCF drawers. The calculations were carried out without considering the leakage. The results of the newly developed Tone's method and the subgroup method are compared to those of TRIPOLI-4® Monte Carlo continuous energy references, which are obtained by using TRIPOLI-4® Version 4.9.0 code with the CEA2005 V5.1.2 library. In these calculations, both Tone's method and subgroup method are based on one-

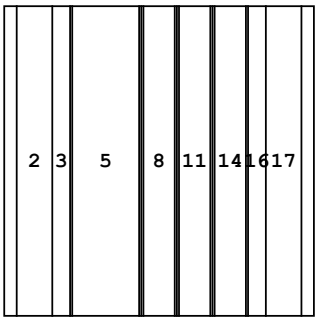


| | | |
|---|---|---|
| 1 | Matrix & Drawer side wall | 0.22225 |
| 2 | U3O8 plate | 0.635 |
| 3 | Depleted uranium | 0.3175 |
| 4 | Can wall | 0.0381 |
| 5 | Sodium | 1.1938 |
| 6 | Can wall | 0.0381 |
| 7 | Can wall | 0.0381 |
| 8 | ZPPR-Pu fuel | 0.5588 |
| 9 | Can wall | 0.0381 |
| 10 | Can wall | 0.0381 |
| 11 | Sodium | 0.5588 |
| 12 | Can wall | 0.0381 |
| 13 | Can wall | 0.0381 |
| 14 | Na2CO3 | 0.5588 |
| 15 | Can wall | 0.0381 |
| 16 | Fe2O3 | 0.3175 |
| 17 | U3O8 plate | 0.635 |
| 18 | Matrix & Drawer side wall | 0.22225 |

Fig. 1: 1D model of the SCF drawer. The widths of plates are given in cm. Numbering for can walls and structure materials are omitted.

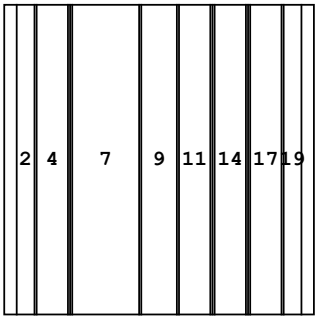


| | | |
|---|---|---|
| 1 | Matrix & Drawer side wall | 0.22225 |
| 2 | Fe2O3 plate | 0.3175 |
| 3 | Can wall | 0.0381 |
| 4 | ZPPR-Pu fuel | 0.5588 |
| 5 | Can wall | 0.0381 |
| 6 | Can wall | 0.0381 |
| 7 | Sodium | 1.1938 |
| 8 | Can wall | 0.0381 |
| 9 | U3O8 plate | 0.635 |
| 10 | Can wall | 0.0381 |
| 11 | Na2CO3 | 0.5588 |
| 12 | Can wall | 0.0381 |
| 13 | Can wall | 0.0381 |
| 14 | Sodium | 0.5588 |
| 15 | Can wall | 0.0381 |
| 16 | Can wall | 0.0381 |
| 17 | ZPPR-Pu fuel | 0.5588 |
| 18 | Can wall | 0.0381 |
| 19 | Fe2O3 plate | 0.3175 |
| 20 | Matrix & Drawer side wall | 0.22225 |

Fig. 2: 1D model of the DCF drawer. The widths of plates are given in cm. Numbering for can walls and structure materials are omitted.

dimensional collision probability solver. The flux solver is one-dimensional IDT flux calculator based on the method of characteristics with linear flux expansion [18, 19].

Table I shows the multiplication factors in the SCF drawer calculations by the two self-shielding methods. Both subgroup and Tone's method agree well with TRIPOLI-4® with error in $k_{eff}$ smaller than 50 pcm. The difference in $k_{eff}$ between the two methods is 64 pcm. We remark that the difference between the two methods in the SCF drawer calculation is more important than those in the SFR fuel-cell and assembly calculations [4]: they are respectively 9 pcm and 25 pcm for these two cases. The number of CP matrix calculations required in self-shielding calculation is also given in Table I. As expected, Tone's method reduces largely the number of CP matrix calculations and therefore the CPU time. The subgroup method requires $\sim$ 43 times more CP calculations and $\sim$ 10 times more CPU time than Tone's method.

Table II shows the multiplication factors in the DCF drawer calculations. Both subgroup and Tone's method agree

TABLE I: SCF drawer calculations: $k_{eff}$ and CPU time

| Options | $k_{eff}^{(a)}$ | $\Delta k_{eff}^{(b)}$ | $\Delta\rho^{(b)}$ | CPU$^{(c)}$ | CPs$^{(d)}$ |
|---|---|---|---|---|---|
| SG | 1.13630 | 22 | 17 | 64 | 204936 |
| Tone | 1.13566 | -42 | -32 | 6 | 4662 |

$^{(a)}$ TRIPOLI-4® reference for $k_{eff}$ is 1.13608 ± 4 pcm;
$^{(b)}$ discrepancy in pcm;
$^{(c)}$ CPU time in flux and self-shielding calculations (sec);
$^{(d)}$ total number of the CP calculations.

TABLE II: DCF drawer calculations: $k_{eff}$ and CPU time

| Options | $k_{eff}^{(a)}$ | $\Delta k_{eff}^{(b)}$ | $\Delta\rho^{(b)}$ | CPU$^{(c)}$ | CPs$^{(d)}$ |
|---|---|---|---|---|---|
| SG | 1.62178 | -16 | -7 | 65 | 193462 |
| Tone | 1.62140 | -54 | -21 | 6 | 4625 |

$^{(a)}$ TRIPOLI-4® reference for $k_{eff}$ is 1.62194 ± 7 pcm;
$^{(b)}$ discrepancy in pcm;
$^{(c)}$ CPU time in flux and self-shielding calculations (sec);
$^{(d)}$ total number of the CP calculations.

well with TRIPOLI-4® with error in $k_{eff}$ smaller than 60 pcm. The difference in $k_{eff}$ between the two methods is 38 pcm, which is smaller than that in the SCF calculations. Similar to the SCF calculations, the subgroup method requires ~ 41 times more CP calculations and ~ 10 times more CPU time than Tone's method.

Figures 3 and 4 present the discrepancies in $^{238}$U absorption rates of the SCF calculations respectively in pcm and in percentage. The results were computed in 1968 groups and showed in 33 group mesh, see APPENDIX for the description of the 33-group energy mesh. We observe that the subgroup method agrees very well with TRIPOLI-4® with error in absorption rates smaller than 6 pcm or less than 5% in energy groups the contributions of which are significant. With Tone's method, the spectrum is similar to that of the subgroup method for groups 1 to 15. However, for groups 16 to 25, there are cancellations of errors in plates 2, 3 and 17. The maximum error in absorption rates can reach 30 pcm or 8% in plate 3, which consists of uranium metal.

Our explication is that Tone's method is based on heterogeneous-homogeneous equivalence through an equivalent cross section. In a region containing pure metal material without moderators, the background cross section $\sigma_{bxi}^{g}$ in Eq. (13) is close to zero, and the equivalent cross section is dominated by the escape cross section $\sigma_{exi}^{g}$. For example, group 20 in the 33-group mesh contains the groups from 1168 to 1228 of the 1968-group mesh. For $^{238}$U in plate 3, the averaged $\sigma_{bxi}^{g}$ is 0.056 barns and the averaged $\sigma_{exi}^{g}$ is 17.891 barns. The averaged equivalent cross section $\sigma_{0xi}^{g}$ changes from 0.056 barns for IHM situation to 17.948 barns for heterogeneous system, the second value is 318 times of the first value. As a comparison, for $^{238}$U in plate 17 where the material is $U_3O_8$, the averaged $\sigma_{bxi}^{g}$ is 10.304 barns and the averaged $\sigma_{exi}^{g}$ is 23.116 barns. The averaged value of $\sigma_{0xi}^{g}$ changes from 10.304 barns for IHM situation to 33.421 barns for heterogeneous system, the second value is 3.24 times of the first value. We see that in a pure metal material, the equivalent cross section obtained for the heterogeneous system is far away from the homogeneous background cross section; in a material with moderators, the equivalent cross section obtained for the heterogeneous system is relatively close to the homogeneous background cross section. That is why the heterogeneous-homogeneous equivalence is less precise for a pure metal material than that for a material with moderators. Since the self-shielded cross sections are determined by iterations until the desired convergence is achieved. The less precise equivalence of $^{238}$U in plate 3 can have influences on the other regions, such as plates 2 and 17.

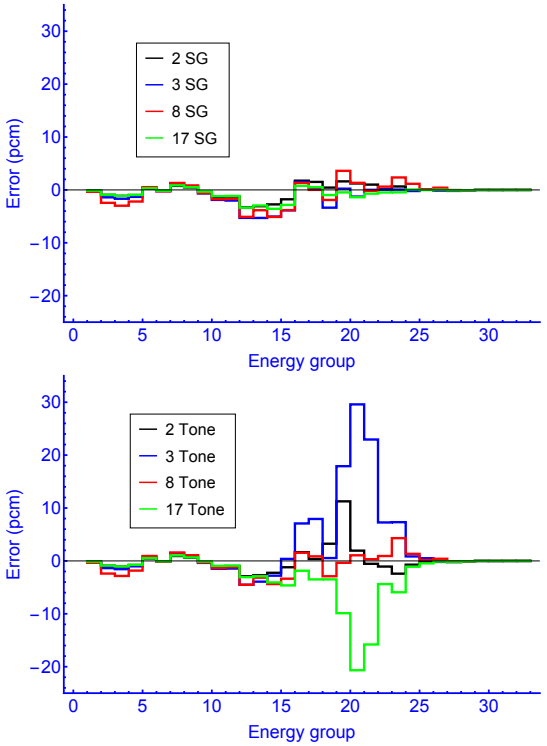


Fig. 3: $^{238}$U absorption rate discrepancies in pcm in SCF drawer calculations.

Figures 5, 6 and 7 show respectively the discrepancies in $^{238}$U production rates, $^{239}$Pu absorption rates and $^{239}$Pu production rates with respect to the Monte Carlo reference in the SCF calculations. These figures show that Tone's method gives equivalent results to the subgroup method.

Figures 8 and 9 present the discrepancies in $^{238}$U absorption rates of the DCF drawer calculations respectively in pcm and in percentage. We see that both subgroup and Tone's method agree well with TRIPOLI-4®. With the subgroup method, the error in absorption rates is smaller than 4 pcm or less than 5% in energy groups whose contributions are significant. As to Tone's method, the error in absorption rates is smaller than 8 pcm or less than 8% in energy groups whose contributions are significant. Tone's method gives slightly less precise results in groups 16 to 24 compared to the subgroup method. This may result from the use of the NR approximation in Tone's method. In DCF drawer, the plates are thin and

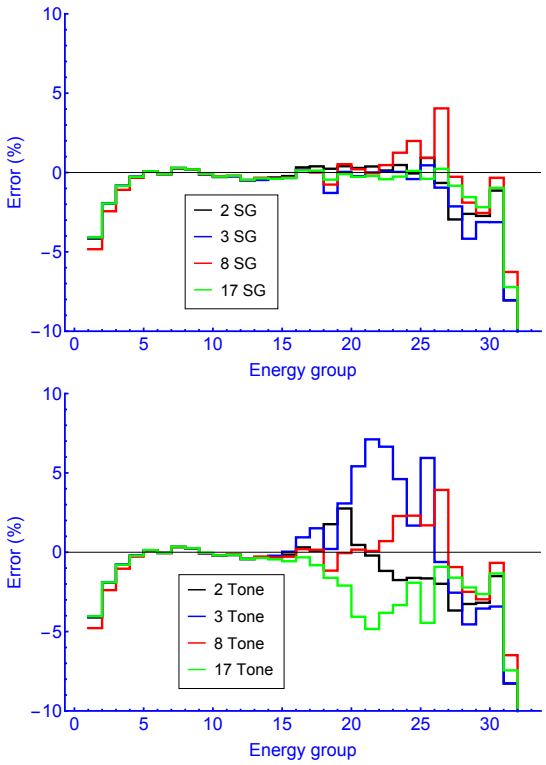


Fig. 4: $^{238}$U absorption rate discrepancies in percentage in SCF drawer calculations.

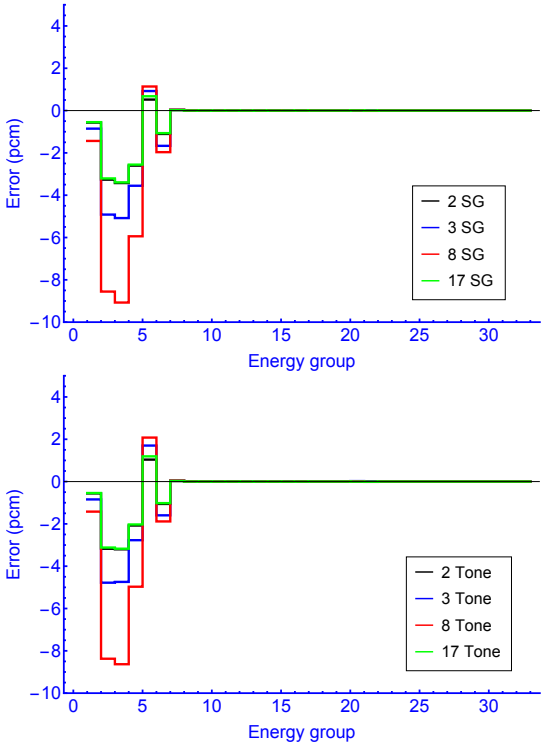


Fig. 5: $^{238}$U production rate discrepancies in SCF drawer calculations.

closely coupled. Hence the actual multigroup sources may be influenced by the other plates in the drawer, and the NR approximation is less precise in this case. But one has to admit that Tone's method, with its use of the NR approximation and Tone's approximation, gives equivalent precision to the subgroup method, which uses the real multigroup sources and the collision probability matrix per subgroup.

Figures 10, 11 and 12 show respectively the discrepancies in $^{238}$U production rates, $^{239}$Pu absorption rates and $^{239}$Pu production rates with respect to the Monte Carlo reference in the DCF calculations. These figures show that Tone's method gives equivalent results to the subgroup method.

## IV. CONCLUSIONS

In this paper we have presented a new resonance self-shielding method based on Tone's method. This method distinguishes from the Tone's methods of the previous studies by utilizing the mathematical probability tables as quadrature formulas in calculating the effective cross sections. The new method has been applied to the ZPPR drawer calculations. The numerical results show that, in the DCF drawer calculations, Tone's method obtains similar precision than the subgroup method, even though the simplified assumptions have been adopted. In the SCF drawer calculation, Tone's method is less precise than the subgroup method due to the pure metal material in plate 3. The heterogeneous-homogeneous equivalence is less precise in case of the pure metal material, because the equivalent cross section is rather different from the homogeneous background cross section.

The numerical results also show the superior efficiency of Tone's method compared to the subgroup method. Thanks to the adoption of the simplified models, the NR approximation for the slowing down source and Tone's approximation for the group collision probabilities, Tone's method largely reduces the required number of CP computations, resulting in an important gain in the CPU time.

## V. ACKNOWLEDGMENTS

The authors are immensely grateful to Dr Richard Sanchez for many fruitful discussions. We would also like to show our particular gratitude to Dr Yi-Kang Lee for his help in running the TRIPOLI-4® calculations of ZPPR benchmarks.

APOLLO3® is a registered trademark of CEA. We gratefully acknowledge AREVA and EDF for their long term partnership and their support.

TRIPOLI-4® is a registered trademark of CEA. We gratefully acknowledge EDF for their long term partnership and AREVA for their support.

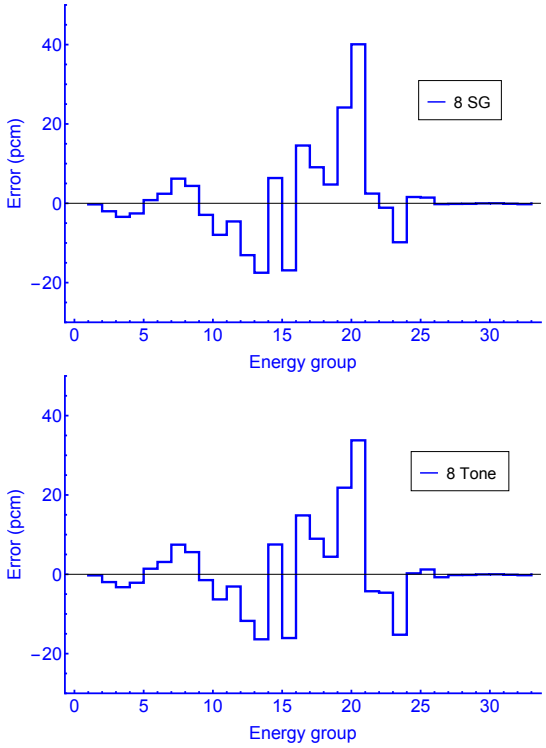


Fig. 6: $^{239}$Pu absorption rate discrepancies in SCF drawer calculations.

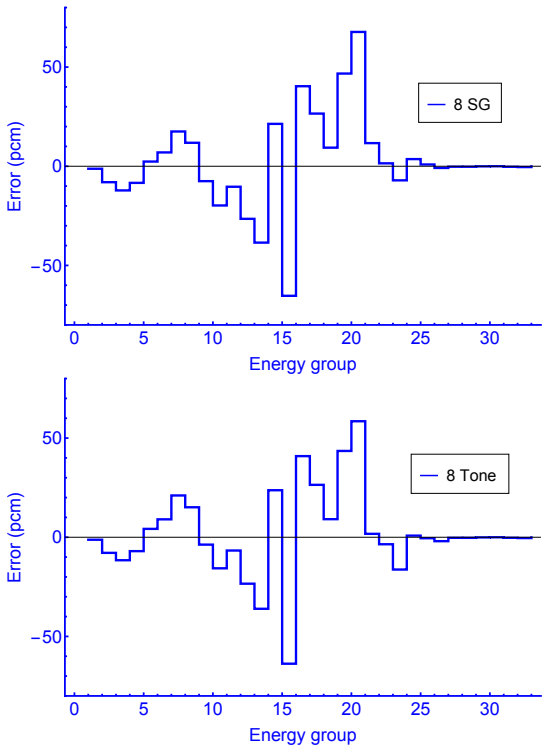


Fig. 7: $^{239}$Pu production rate discrepancies in SCF drawer calculations.

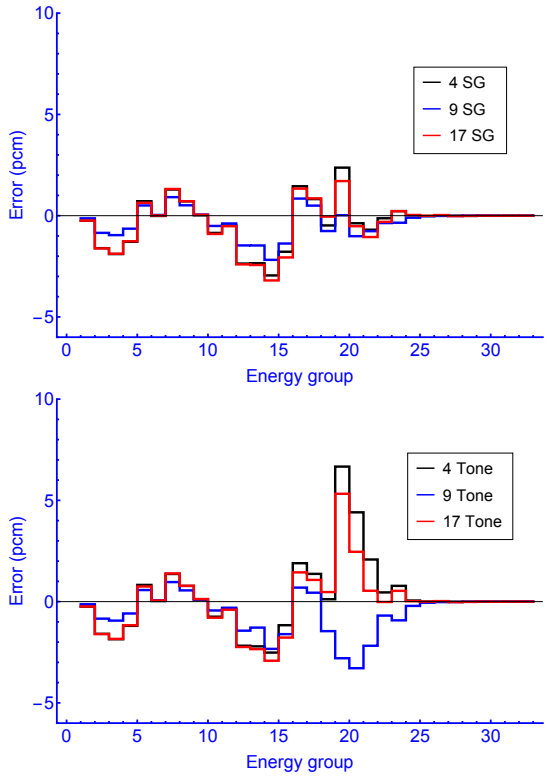


Fig. 8: $^{238}$U absorption rate discrepancies in pcm in DCF drawer calculations.

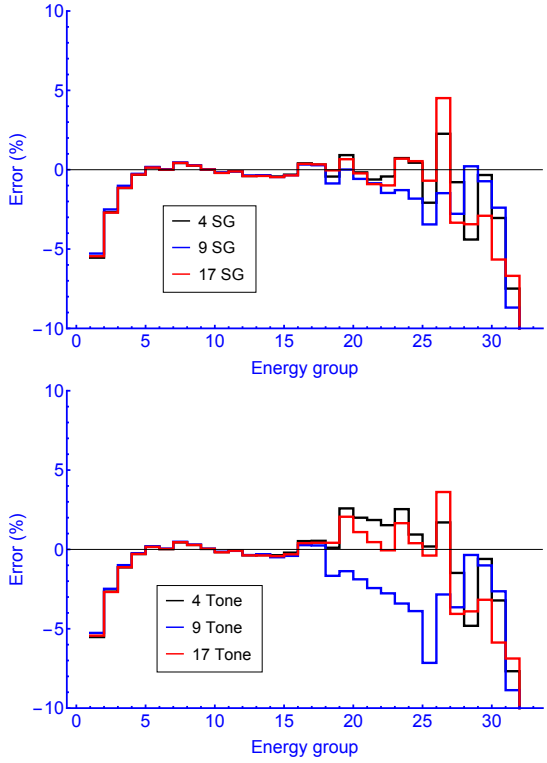


Fig. 9: $^{238}$U absorption rate discrepancies in percentage in DCF drawer calculations.

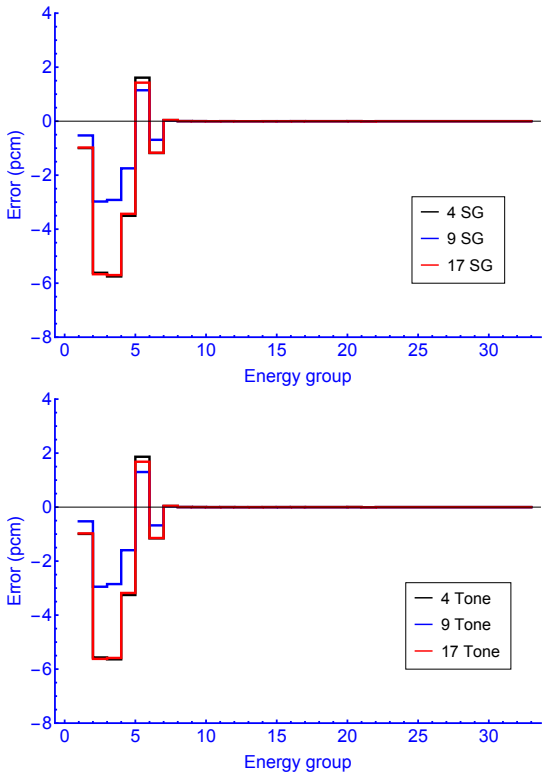


Fig. 10: $^{238}$U production rate discrepancies in DCF drawer calculations with the average fission spectrum.

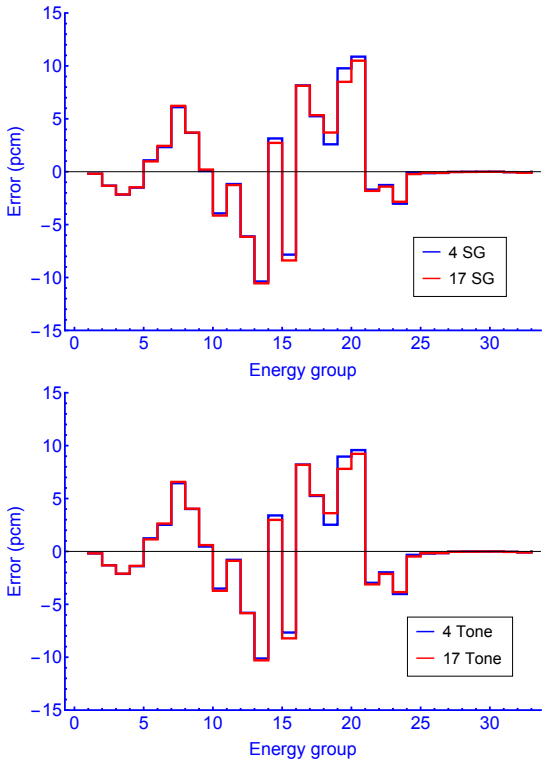


Fig. 11: $^{239}$Pu absorption rate discrepancies in DCF drawer calculations with the average fission spectrum.

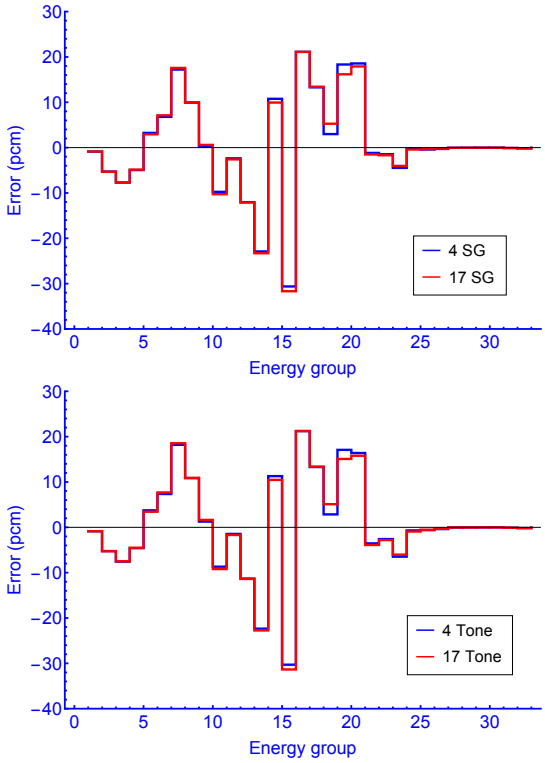


Fig. 12: $^{239}$Pu production rate discrepancies in DCF drawer calculations with the average fission spectrum.

## APPENDIX: THE 33-GROUP ENERGY MESH

The 33-group energy mesh

| Group | Upper bound (eV) | Group | Upper bound (eV) |
|---|---|---|---|
| 1 | $1.964033 \times 10^{+7}$ | 18 | $3.354626 \times 10^{+3}$ |
| 2 | $1.000000 \times 10^{+6}$ | 19 | $2.034684 \times 10^{+3}$ |
| 3 | $6.065307 \times 10^{+6}$ | 20 | $1.234098 \times 10^{+3}$ |
| 4 | $3.678794 \times 10^{+6}$ | 21 | $7.485183 \times 10^{+2}$ |
| 5 | $2.231302 \times 10^{+6}$ | 22 | $4.539993 \times 10^{+2}$ |
| 6 | $1.353353 \times 10^{+6}$ | 23 | $3.043248 \times 10^{+2}$ |
| 7 | $8.208500 \times 10^{+5}$ | 24 | $1.486254 \times 10^{+2}$ |
| 8 | $4.978707 \times 10^{+5}$ | 25 | $9.166088 \times 10^{+1}$ |
| 9 | $3.019738 \times 10^{+5}$ | 26 | $6.790405 \times 10^{+1}$ |
| 10 | $1.831564 \times 10^{+5}$ | 27 | $4.016900 \times 10^{+1}$ |
| 11 | $1.110900 \times 10^{+5}$ | 28 | $2.260329 \times 10^{+1}$ |
| 12 | $6.737947 \times 10^{+4}$ | 29 | $1.370959 \times 10^{+1}$ |
| 13 | $4.086771 \times 10^{+4}$ | 30 | $8.315287 \times 10^{+0}$ |
| 14 | $2.478752 \times 10^{+4}$ | 31 | $4.000000 \times 10^{+0}$ |
| 15 | $1.503439 \times 10^{+4}$ | 32 | $5.400000 \times 10^{-1}$ |
| 16 | $9.118820 \times 10^{+3}$ | 33 | $1.000000 \times 10^{-1}$ |
| 17 | $5.530844 \times 10^{+3}$ | | $1.000010 \times 10^{-5}$ |

## REFERENCES

1. H. GOLFIER et al., "APOLLO3: a common project of CEA, AREVA and EDF for the development of a new deterministic multi-purpose code for core physics analysis," in "*Proc. Int. Conf. on Mathematics, Computational Methods & Reactor Physics (M&C 2009)*," Saratoga Springs, New York, May 3-7 (2009).
2. D. SCHNEIDER et al., "APOLLO3®: CEA/DEN Deterministic Multi-purpose Code for Reactor Physics Analysis," in "*Proc. PHYSOR 2016*," Sun Valley, ID, May 1-5, (2016).
3. G. RIMPAULT, "Algorithmic features of the ECCO cell code for treating heterogeneous fast reactor assemblies," in "*Proc. Int. Conf. Mathematics and Computations, Reactor Physics and Environmental Analyses*," Portland, Oregon, April 30-May 4 (1995).
4. L. MAO and I. ZMIJAREVIC, "Resonance self-shielding methods for fast reactor calculations - Comparison of a new Tone's method with the subgroup method in APOLLO3®," *submitted to Nucl. Sci. Eng.* (2016).
5. P. RIBON and J.-M. MAILLARD, "Les tables de probabilités. Application au traitement des sections efficaces pour la neutronique," Tech. Rep. CEA-N-2485, Commissariat à l'Energie Atomique (1986).
6. M. COSTE-DELCLAUX, "A nuclear data processing system for transport depletion and shielding codes," in "*Proc. Int. Conf. on the Physics of Reactors "Nuclear Power: A Sustainable Resource" (PHYSOR 2008)*," Interlaken, Switzerland, September 14-19 (2008).
7. C.M. DIOP et al., "Review of the TRIPOLI-4 Monte Carlo Transport Code," in "*Proc. of the Int. Cong. on Advances in Nuclear Power Plants (ICAPP 2007)*," Nice Acropolis, France, May 13-18 (2007).
8. T. TONE, "A numerical study of heterogeneity effects in fast reactor critical assemblies," *J. Nucl. Sci. Technol.*, **12[8]**, 467 (1975).
9. M. ISHIKAWA, "Consistency evaluation of JUPITER experiment and analysis for large FBR cores," in "*Proc. Int. Conf. on the Physics of Reactors (PHYSOR 96)*," Mito, Ibaraki, Japan, September 16-20 (1996).
10. H. YU, T. ENDO, and A. YAMAMODO, "Resonance Calculation for Large and Complicated Geometry Using Tone's Method by Incorporating the Method of Characteristics," *J. Nucl. Sci. Technol.*, **48[3]**, 330 (2011).
11. C. LEE and W. YANG, "An Improved Resonance Self-Shielding Method for Heterogeneous Fast Reactor Assembly and Core Calculations," in "*Proc. M&C 2013*," Sun Valley, Idaho, May 5-9 (2013).
12. A. WEINBERG and E. WIGNER, *The physical theory of neutron chain reactors*, University of Chicago Press, Chicago (1958).
13. I. CARLVIK, "The Dancoff Correction in Square and Hexagonal Lattices," *Nucl. Sci. Eng.*, **29**, 325 (1967).
14. G. CHIBA, "A combined method to evaluate the resonance self-shielding effect in power fast reactor fuel calculation," *J. Nucl. Sci. Technol.*, **40[7]**, 537 (2003).
15. M. ISHIKAWA, T. IKEGAMI, and T. SANDA, "ZPPR Benchmarks for Large LMFBR Core Physics from JUPITER Cooperative Program Between United States and Japan," *Nucl. Sci. Eng.*, **178**, 335–349 (2014).
16. J. BUSSAC and P. REUSS, *Traité de neutronique*, Hermann, Paris (1985).
17. R. STAMMĹER and M. ABBATE, *Methods of Steady-State Reactor Physics in Nuclear Design*, Academic Press, London (1983).
18. I. ZMIJAREVIC, "Multidimensional Discrete Ordinates Nodal and Characteristics Methods for APOLLO2 code," in "*Proc. Int. Conf. on Mathematics and Computation, Reactor Physics and Environmental Analysis in Nuclear Applications (M&C 1999)*," Madrid, Spain, Sept. 27-30 (1999).
19. E. MASIELLO, R. SANCHEZ, and I. ZMIJAREVIC, "New Numerical Solution with the Method of Short Characteristics for 2-D Heterogeneous Cartesian Cells in the APOLLO2 code: Numerical Analysis and Tests," *Nucl. Sci. Eng.*, **161**, 257 (2009).